Characterization of l-phenylalanine metabolism to acetophenone and 1-phenylethanol in the flowers of Camellia sinensis using stable isotope labeling

Running title: Volatiles in *Camellia sinensis* flowers

Corresponding author

Name: Naoharu Watanabe

Mailing address: *Graduate School of Science and Technology, Shizuoka University, 836 Ohya, Suruga-ku, Shizuoka 422-8529, Japan*

Tel: +8154-2384870; fax: +8154-2384870.

Email address: acnwata@ipc.shizuoka.ac.jp

Title: Characterization of L-phenylalanine metabolism to acetophenone and 1-phenylethanol in the flowers of *Camellia sinensis* using stable isotope labeling

Authors: Fang Dong [a, #], Ziyin Yang [a, #], Susanne Baldermann [a], Yutaka Kajitani [b], Shogo Ota [b], Hisae Kasuga [b], Yumi Imazeki [b], Toshiyuki Ohnishi [a], Naoharu Watanabe [a, *]

***Affiliation*:**

[a] *Graduate School of Science and Technology, Shizuoka University, 836 Ohya, Suruga-ku, Shizuoka 422-8529, Japan*

[b] *Corporate Research & Development Division, Takasago International Corporation,* 4-11, *Nishiyawata 1-chome, Hiratsuka City, Kanagawa 254-0073 Japan*

[#] These authors contributed equally to this work. [*] Corresponding author. Tel: +8154-2384870; fax: +8154-2384870. *Email address:* acnwata@ipc.shizuoka.ac.jp (N. Watanabe).

Summary

Acetophenone (AP) and 1-phenylethanol (1PE) are the two major endogenous volatile compounds in flowers of *Camellia sinensis* var. Yabukita. Until now no information has been available on the biosynthesis of AP and 1PE in plants. Here we propose that AP and 1PE are derived from L-phenylalanine (L-Phe), based on feeding experiments using stable isotope-labeled precursors L-[$^{2}H_{8}$]Phe and L-[$^{13}C_{9}$]Phe. The subacid conditions in the flowers result in more hydrogenation than dehydrogenation in the transformation between AP and 1PE. Due to the action of some enzyme(s) responsible for the formation of (*R*)-1PE from AP in the flowers, (*R*)-1PE is the dominant endogenous steroisomer of 1PE. The modification of 1PE into nonvolatile glycosidic forms is one of the reasons for why only a little 1PE is released from the flowers. The levels of AP, 1PE, and glycosides of 1PE increase during floral development, whereas the level of L-Phe decreases. These metabolites occur mostly in the anthers.

Keywords: Acetophenone; *Camellia sinensis*; L-phenylalanine; 1-phenylethanol; precursor

Abbreviations:

AIP, 2-aminoindan-2-phosphonic acid; AP, acetophenone; CA, cinnamic acid; HPPA, 3-hydroxy-3-phenylpropionic acid; MSTFA, N-methyl-N-(trimethylsilyl) trifluoroacetamide; PAA, phenyllactic acid; PAL, phenylalanine ammonia-lyase; 1-PE, 1-phenylethanol; L-Phe, L-phenylalanine; PPA, phenylpyruvic acid; PVPP, polyvinylpolypyrrolidone

Introduction

Plants synthesize and release a large variety of volatile organic compounds, which can be viewed as the plant's interface with the surrounding environment. These volatile compounds are released from flowers, leaves, fruits, or roots into the atmosphere or soil, allowing the plant to interact with other organisms while remaining anchored to the ground (Negre-Zakharov et al., 2009). The volatile compounds emitted from vegetative parts, especially after herbivore attack, appear to protect plants by deterring herbivores and by attracting the enemies of herbivores, whereas floral volatiles serve as attractants for species-specific pollinators (Pichersky and Gershenzon, 2002). The volatile compounds emitted from flowers include fatty acid derivatives, benzenoids, phenylpropanoids, isoprenoids, and nitrogen- and sulphur-containing compounds (Knudsen et al., 1993). Isoprenoids are formed by geranyl pyrophosphate/geranylgeranyl pyrophosphate pathways, whereas most phenylpropanoids and benzenoids are derived from shikimic acid (Pichersky et al., 2006). The biosynthetic pathways of many volatile phenylpropanoids and benzenoids (including phenylacetaldehyde, 2-phenylethanol, phenylethylbenzoate, benzaldehyde, benzylalcohol, benzylbenzoate, eugenol, and isoeugenol) have been intensively investigated in plants (Boatright et al., 2004). However, the plant biosynthetic pathways of some other volatile phenylpropanoids/benzenoids, including acetophenone (AP) and 1-phenylethanol (1PE), remain unknown. In the present study, we found that AP and 1PE are the two major endogenous volatile compounds in flowers of *Camellia sinensis* (tea), which allowed us to use the *C. sinensis* flowers as a model for studying the biosynthesis of these two volatile compounds. By supplying stable isotope-labeled precursors to the flowers, we found evidence that AP and 1PE are derived from L-phenylalanine (L-Phe). We investigated the stereochemistry of 1PE and its transformation from AP. In addition, we investigated the distribution of the two compounds and their precursors

in floral organs, their emission from flowers, and the changes in their endogenous concentrations during floral development.

Materials and methods

Samples

The leaves and flowers of *C. sinensis* var. Yabukita, which is the most popular variety of tea in Japan, were obtained from tea fields at the Center for Education and Research in Field Sciences, Shizuoka University (Shizuoka, Japan) between October and December in 2008, 2009, 2010, and 2011. Flower development was divided into 3 stages: at stage 1 the flower buds are closed, at stage 2 the flower is half open, and at stage 3 the flower is fully open (Figure S1, Supplementary Materials).

Feeding of stable isotope-labeled compounds to cut flowers and identification of products

Cut flowers at stage 1 were kept in an incubator with a 12-h light/12-h dark photoperiod at 70% humidity and 18-20ºC. Individual flowers were placed in one of the following solutions: (1) water (as control); (2) 12 mM L-[a,b,b,2,3,4,5,6-$^{2}H_{8}$]Phe (L-[$^{2}H_{8}$]Phe, deuterium atom ≥ 98%, Cambridge Isotope Laboratories, Inc.); (3) 12 mM L-U-$^{13}C_{9}$-Phe (L-[$^{13}C_{9}$]Phe, U-$^{13}C_{9}$, 97-99%, Cambridge Isotope Laboratories, Inc.); (4) 12 mM sodium acetate-1-^{13}C (^{13}C atom ≥ 99%, Isotec Corporation); (5) 12 mM sodium acetate-2-^{13}C (^{13}C atom ≥ 99%, Isotec Corporation); and (6) 12 mM sodium acetate-$^{13}C_{2}$ (^{13}C atom ≥ 99%, Isotec Corporation). After 18-20 h (while the flower developed from stage 1 to stage 3), the headspace volatile compounds were collected using solid phase microextraction (Supelco Inc.) with 100 μm polydimethylsiloxane coated fiber (2 h sampling for each flower, Figure S2, Supplementary Materials).

To identify the nonvolatile products of the isotope-labeled compounds used in the feeding experiments, N-methyl-N-(trimethylsilyl) trifluoroacetamide (MSTFA) derivatization was used. Table S1 (Supplementary Materials) shows the MSTFA derived products of nonlabeled authentic standards and their molecular weights, and characteristic ions based on analysis of gas chromatography (GC) time-of-flight (TOF) mass spectrometry (MS).

To identify the labeled *trans*-cinnamic acid (CA) and phenyllactic acid (PAA) products, 500 mg or 800 mg (fresh weight) of finely powdered floral tissues crushed by a Multi-Beads Shocker (2,000 rpm, 15 sec, Yasui Kikai Corporation, Japan) were extracted with 4 mL of cold methanol by vortexing for 2 min followed by an ultrasonic extraction in ice cold water for 10 min. Each extract was mixed with 4 mL of cold chloroform and 1.6 mL of cold water for phase separation, and the resulting upper layer was filtered through a 0.2 μm membrane filter, dried, and then redissolved in 0.5 mL of water. Five hundred microliter of the extract in water was mixed with 12 μL of 0.25 N hydrochloric acid and extracted twice with 1.0 mL of ethyl acetate. The ethyl acetate extract was dried, and derivatized with 80 μL of MSTFA at 37°C for 60 min, and then centrifuged. The MSTFA derivates were then analyzed by a GC-MS QP5000 (Shimadzu), which was controlled by a Class-5000 work station. The injector temperature was 230°C, splitless mode was used with a splitless time of 1 min, and helium was the carrier gas with a velocity 1.5 mL/min. The HP-1MS column (Agilent Technologies, 30 m × 0.25 mm × 0.25 μm) was used with an initial temperature of 80°C for 3 min, a ramp of 15°C/min to 300°C, and then a hold at 300°C for 15 min. The MS analyses were carried out in SIM mode.

To identify the labeled phenylpyruvic acid (PPA) product, 500 mg (fresh weight) of finely powdered floral tissues were homogenized on ice with 5 mL of cold pH 6.0 buffer (ammonium acetate- acetic acid), and then centrifuged (26,740 *g*, 4°C, 15 min). The supernatant was diluted

with water to 40 mL, and then passed through a 6 mL Supelclean Envi-Chrom P column (Supelco), afterwards eluted by 6 mL of acetonitrile. The acetonitrile elute was dried, and then redissolved in 0.5 mL of water. Five hundred microliter of the extract in water was mixed with 12 μL of 0.25 N hydrochloric acid and extracted twice with 1.0 mL of ethyl acetate. The ethyl acetate extract was dried, and derivatized with 80 μL of MSTFA at 37°C for 60 min, and then centrifuged. The MSTFA derivates were analyzed by GC-MS in SIM mode as described above.

To identify endogenous volatile products, finely powdered floral tissues (500 mg fresh weight) were extracted for 17 h in the dark with 2 mL of hexane: ethyl acetate (1:1). The extract was then filtered through a short plug of anhydrous sodium sulfate and 1 μL of the filtrate was subjected to GC-MS analysis. The injector temperature was 230°C, splitless mode was used with a splitless time of 1 min, and helium was the carrier gas with a velocity 1.6 mL/min. The SUPELCOWAX^{TM} 10 column (Supelco Inc., 30 m × 0.25 mm × 0.25 μm) was used with an initial temperature of 40°C, a ramp of 5°C/min to 240°C, and then a hold at 240°C for 15 min. The MS analyses were carried out in full scan (mass range *m/z* 70–200) and SIM modes.

To analyze volatile compounds collected by SPME, desorption of volatiles from the fiber was placed in hot GC injector at 230°C, for 1 min. The GC-MS conditions are same as described above.

Inhibition experiments and identification of volatile products

The 0.02, 0.2, and 2 mM monohydrate 2-aminoindan-2-phosphonic acid (AIP, kindly provided by Prof. Jerzy Zoń) , a potent inhibitor of phenylalanine ammonia-lyase (PAL), together with L-[$^{2}H_{8}$]Phe and L-[$^{13}C_{9}$]Phe as described above were supplied to the cut flowers at stage 1, respectively. The AIP was obtained according to the literature procedure (Zoń and Amrhein,

1992). After 18-20 h (while the flower developed from stage 1 to stage 3), finely powdered floral tissues (350 mg fresh weight) were extracted for 17 h in the dark with 1.5 mL of hexane: ethyl acetate (1:1). The extract was then filtered through a short plug of anhydrous sodium sulfate and 1 μL of the filtrate was subjected to GC-MS analysis as described above.

Investigations on exchange reaction of deuterium during feeding experiments

To investigate whether the deuterium of labeled metabolites in the feeding experiments is replaced by hydrogen, the following in *vitro* and in *vivo* experiments were carried out. For in *vitro* experiments, 2 mg of non-labeled AP was incubated in 0.5 mL of methanol and methanol-d_4 (D, 99.8%, Cambridge Isotope Laboratories, Inc.), respectively, under the same condition with the feeding experiments as described above. After 18 h-incubation, the solution was diluted with hexane: ethyl acetate (1:1) by 1000 times, and dried over anhydrous sodium sulfate. One microliter of the filtrate was subjected to GC-MS analysis as described above. Ten milligram of non-labeled CA and 3-hydroxy-3-phenylpropionic acid (HPPA) were incubated in 0.5 mL of methanol-d_4, respectively, under the same condition with the feeding experiments. After 18 h-incubation, the solution was analyzed by ^{1}H NMR (JEOL 270 MHz). In addition, 150 mg/L of non-labeled CA and HPPA in methanol and methanol-d_4 were prepared. After 18 h-incubation, the solution was analyzed by Agilent Technologies 1200 series HPLC-JEOL The AccuTOFLC-plus JMS-T100LP.

For in *vivo* experiments, individual flowers at stage 1 were under the same condition with the feeding experiments as described above, and placed in one of the following solutions: (1) water; (2) 12 mM nonlabeled L-Phe in water; (3) deuterium oxide (D, 99.9%, Cambridge Isotope Laboratories, Inc.); (4) 12 mM nonlabeled L-Phe in deuterium oxide. After 18-20 h (while the

flower developed from stage 1 to stage 3), the endogenous volatile products were extracted and analyzed by GC-MS as described above.

Analysis of endogenous and emitted AP and 1PE from C. sinensis flowers

To analyze endogenous volatile compounds at each floral stage and from each floral organ, finely powdered floral tissues (330 mg fresh weight) were extracted for 17 h in the dark with 1.5 mL of diethyl ether containing 25.2 nmol of ethyl *n*-decanoate as an internal standard. The extract was then filtered through a short plug of anhydrous sodium sulfate and 1 μL of the filtrate was subjected to GC-MS analysis. Samples were analyzed using an Agilent 7890 gas chromatograph with a 5975 mass spectrometer, and the system was controlled by a GC/MSD Chemstation. The injector temperature was 240°C, splitless mode was used with a splitless time of 1 min, and helium was the carrier gas with a velocity 1.2 mL/min. The SUPELCOWAX^{TM} 10 column (Supelco Inc., 30 m × 0.25 mm × 0.25 μm) was used with an initial temperature of 40°C, a ramp of 5°C/min to 250°C, and then a hold at 250°C for 15 min. The MS analyses were carried out in full scan (mass range *m/z* 70–200) and SIM modes. Electron impact ionisation at energy 70 eV was used for every measurement. The ion source and quadrupole analyzer temperatures were fixed at 230°C and 150°C, respectively. All volatile compounds were identified by comparing their retention times and mass spectra with those of authentic compounds. Quantification was performed using calibration curves generated from individual authentic standards.

The volatiles emitted from each flower were collected using the MonoTrap^{TM} absorption system with a set of 5 disks and 4 rods. The volatiles were collected for 3 h from flowers at each developmental stage. The trapped compounds were eluted from the MonoTrap^{TM} with 1 mL

dichloromethane containing 10 μL 5-nonanone (10 mg/L in ethanol) and 10 μL 3-octanone (1000 mg/L in ethanol) as internal standards. The eluate was concentrated to 50 μL with a Kuderna-Danish concentrator at 45ºC, further concentrated under N_2 gas, and then 2 μL of the concentrated solution was subjected to GC-MS analysis. The settings were as follows: injector temperature 250°C, splitless mode with a splitless time of 1.5 min, carrier gas helium with a constant pressure of 108 kPa. The BC-WAX column (GL Science Inc., 50 m × 0.25 mm I.D. × 0.15 μm) was used with initial temperature 35°C for 1.5 min, a ramp of 5°C/min to 170°C, then a ramp 20°C/min to 220°C. The MS analyses were carried out in SIM mode (*m/z* 105 and 120 for AP, *m/z* 107 and 122 for 1PE, *m/z* 99 and 128 for 3-octanone, *m/z* 85 and 142 for 5-nonanone).

Determination of stereochemistry of 1PE

Flowers (10 g fresh weight) were extracted with 50 mL pentane: dichloromethane (1:1) for 24 h, then the suspension was filtered, and the filtrate was dried overnight in anhydrous sodium sulfate. Ten microliter of 3-octanone (1000 mg/L in ethanol) as an internal standard was added to the resultant solution, concentrated to 1 mL with a Kuderna-Danish concentrator at 45ºC and then further concentrated to 500 μL under N_2 gas. For analysis of endogenous 1PE in the flowers, the levels of (*R*)-1PE and (*S*)-1PE were measured using a MDGC/GCMS-2010 system (Shimadzu Corporation) equipped with a Rxi-5ms column (Restek, 30 m × 0.25 mm × 0.25 μm) for the first GC (GC-2010) and a β-DEX225 (chiral column, Supelco, 30 m × 0.25 mm × 0.25 μm) for the second GC (GCMS-QP2010). The conditions of the first GC were as follows: injected volume (of concentrated solution) 2 μL, split ratio 1:10, carrier gas helium with a constant pressure of 225 kPa, initial column temperature 40°C followed by a ramp of 5°C/min to 300°C. The temperatures of the injector, FID detector, and transfer line into the second GC were kept at

290°C, 300°C, and 180°C, respectively. The heart-cut time was from 11.15 to 11.35 min. For the second GC the initial temperature was 50°C for 15 min followed by a ramp of 1.5°C/min to 200°C, with the mass interface and ion source kept at 200°C. The MS analyses were carried out in full scan mode.

To determine the levels of (*R*)- and (*S*)-1PE emitted from flowers, the MDGC/GCMS procedure was similar to that described above with the following differences: For the first GC, 3 μL of the concentrated solution was injected, the splitless mode was used with a splitless time of 1.5 min, and the temperatures were: 40°C for 5 min, a ramp of 5°C/min to 105°C, then a ramp of 10°C/min to 300°C. The temperature of the transfer line was 200°C and the heart-cut time was 15.5–16.2 min. For the second GC the initial temperature was 50°C for 16 min followed by a ramp of 2°C/min to 140°C. The MS analyses were carried out in the SIM mode (*m/z* 79, 107 and 122).

Analysis of glycosides of 1PE

Plant tissues (200 mg fresh weight, finely powdered) were extracted with 1 mL cold methanol by vortexing for 2 min followed by ultrasonic extraction in ice cold water for 10 min. The extracts were mixed with 1 mL cold chloroform and 0.4 mL cold water for phase separation, and the resulting upper layer was dried, and redissolved in 1 mL of water. The resulting solution was mixed with 40 mg polyvinylpolypyrrolidone (PVPP) and centrifuged (16,400 *g*, 4°C, 10 min), and this was repeated with the supernatant. The second supernatant (1 mL) was loaded on an Amberlite XAD-2 column and eluted successively with 5 mL water, 5 mL pentane: dichloromethane (2:1), and 5 mL methanol. The methanol eluate was concentrated in a vacuum, dried under nitrogen gas, redissolved in 0.4 mL of 50 mM citric acid buffer (pH 6.0) containing

10 mg β-primeverosidase (1.12 unit, purchased from Amano Enzyme Inc., Japan) and 0.6 mg β-glucosidase (from almonds, 3.12 unit), and allowed to react at 37°C for 14 h. Sodium chloride (144 mg) was added to the reaction solution, and stood for 15 min. Afterwards 5 nmol of ethyl *n*-decanoate as an internal standard was added. The solution was extracted with 0.4 mL hexane:ethyl acetate (1:1), centrifuged (16,400 *g*, 4°C, 3 min), and the supernatant was dried over anhydrous sodium sulfate. The samples were then analyzed by GC-MS as described above, with some differences. For the 1PE analysis, helium was used as the carrier gas at a flow rate of 1.6 mL/min. The GC temperatures were 60°C for 3 min, ramps of 40°C/min to 180°C followed by 10°C/min to 240°C, then 240°C for 3 min. MS was performed in full scan mode (mass range *m/z* 70–200). For the analyses of (*R*)- and (*S*)-1PE, an InertCap CHIRAMIX (GL Science Inc., 30 m × 0.25 mm × 0.25 μm) was used with helium as the carrier gas at a flow rate of 1.8 mL/min. The temperatures were 40°C for 5 min, a ramp of 3°C/min to 180°C, then 180°C for 10 min. MS was performed in full scan mode (mass range *m/z* 70–200) and SIM mode (*m/z* 77, 79, 107 and 122).

Analysis of L-Phe

Finely powdered plant tissues (100 mg) were extracted with 2 mL cold 70% methanol containing 20 μL of 612.3 μM L-[$^{2}H_{8}$]Phe (dissolved in 70% methanol) as an internal standard by vortexing for 2 min followed by ultrasonic extraction in ice cold water for 10 min, and then centrifuged. The supernatant was filtered through a 0.2 μm membrane filter then diluted 10 × with 70% methanol prior to ACQUITY UPLC-LCT Premier XETM analysis. The sample (2 μL, 4°C) was injected onto a Waters ACQUITY BEH AMIDE column (2.1 × 100 mm, 1.7 μm) which was kept at 40°C. The compounds were eluted using a flow rate of 0.2 mL/min with a

chromatographic gradient of two mobile phases (A: 0.1% aqueous formic acid; B: 0.1% formic acid in acetonitrile). Solvent A was maintained at 10% for 3 min, increased linearly to 30% at 8.0 min, then maintained at 30% for 3 min. The electrospray source and desolvation temperatures were 120°C and 400°C, respectively. The nebulizer gas and desolvation gas flow rates were 50 L/h and 700 L/h, respectively. The sample cone and capillary voltages were 10 V and 3.0 kV, respectively. Spectra were collected in the positive ionization V mode (ES+, *m/z* 100-700).

Extraction and assay of crude enzymes involved in the transformation between AP and 1PE

Finely powdered plant tissues (1 g) were homogenized on ice with 0.3 g PVPP, 20 mg 3-[(3-cholamidopropyl)-dimethylamino]-1-propanesulfonate, and 10 mL cold 100 mM potassium phosphate buffer (pH 7.0) containing 1% glycerol and 1 mM EDTA. The supernatant was centrifuged twice (26,740 *g*, 4°C, 20 min) to remove suspended substances then loaded on a PD-10 desalting column (GE Healthcare Bio-Sciences) and eluted using 10 mM potassium phosphate buffer (pH 7.0) containing 0.1% glycerol and 0.1 mM EDTA. The eluate was used as a crude enzyme solution. The reaction mixture contained 200 μL enzyme solution, 50 μL substrate (0.4 μmol labeled [$^2H_5$] ring-AP (98%, Cambridge Isotope Laboratories, Inc.) or nonlabeled 1PE), 50 μL coenzyme (1.5 μmol, NADPH or $NADP^+$), and 100 μL of 100 mM potassium phosphate buffer (pH 5.0, 5.8, 6.5, or 8.0). The reaction was incubated at 35°C for 45 min. Sodium chloride (144 mg) was added to the reaction solution, and stood for 15 min. Afterwards 5 nmol of ethyl *n*-decanoate as an internal standard was added. The reaction products were extracted with 0.4 mL of hexane:ethyl acetate (1:1), centrifuged (16,400 *g*, 4°C, 3 min), and the supernatant was dried over anhydrous sodium sulfate. Samples were then analyzed by GC-MS as described above.

Results and Discussion

AP and 1PE are derived from L-Phe in C. sinensis flowers

AP is a precursor of compounds in fragrances resembling almond, cherry, jasmine, and strawberry. 1PE is used widely as a fragrance in the cosmetic industry because of its mild floral odor (Suan and Sarmidi, 2004). The synthetic pathways for AP and 1PE in microbes and in chemical reactions are known (Yun et al., 2003; Bailey and Luderer, 2010; Nakata et al., 2010), however the biosynthetic pathways of these two volatile compounds in plants have not yet been elucidated. We found that *C. sinensis* flowers contain much higher amounts of endogenous AP and 1PE than those of *C. sasanqua* (Table S2, Supplementary Materials). Moreover, AP and 1PE were identified as the two major endogenous volatile compounds in *C. sinensis* var. Yabukita flowers (Figure S3, Supplementary Materials). Therefore, *C. sinensis* var. Yabukita was used as a model for studying these two volatile compounds. Sodium acetate may enhance the availability of acetyl coenzyme A, which is an important precursor of secondary metabolites formed from the acetate pathway (Dewich, 2002). Therefore, ^{13}C labeled sodium acetates were used in feeding experiments with cut *C. sinensis* flowers. However, ^{13}C labeled AP and 1PE products were not detected, suggesting that these compounds are not derived from the acetate pathway in *C. sinensis* flowers. The first committed step in the biosynthesis of some volatile phenylpropanoid and benzenoid compounds is the deamination of L-Phe (Dudareva and Pichersky, 2006). Furthermore, it has been proposed that the fungus *Bjerkandera adusta* has a pathway leading from L-Phe to AP *via* CA and HPPA (Lapadatescu et al., 2000, Figure 1). Therefore, we also used deuterium labeled L-Phe (L-[$^2H_8$]Phe) in our feeding experiments (Figure S2, Supplementary Materials). Among the volatile products emitted from the flowers, [$^2H_5$]AP was the dominant isotopologue and [$^2H_6$]AP was detected as a minor isotopologue (Figure S4A, Supplementary

Materials). Labeled 1PE product was not detected due to its low emission from the flowers. Among the endogenous volatile products, [$^2H_5$]AP and [$^2H_5$]-1PE were detected as dominant isotopologues, while [$^2H_6$]AP and [$^2H_6$]-1PE were present as minor isotopologues (Figure 2).

There are several possibilities to result in [$^2H_5$]AP and [$^2H_5$]-1PE formation in the feeding experiments of L-[$^2H_8$]Phe to the cut flowers. One is that the methyl group of AP and 1PE may be provided by other metabolites not by L-Phe. To investigate it, we used L-[$^{13}C_9$]Phe to the feeding experiments (Figure S2, Supplementary Materials) to check whether the product is [$^{13}C_8$]AP or [$^{13}C_7$]AP. If the product is [$^{13}C_7$]AP, the methyl group may come from other metabolites. As consequences, in the endogenous volatile products, [$^{13}C_8$]AP and [$^{13}C_8$]-1PE were detected as dominant isotopologues (Figure 3). Although [$^{13}C_7$]AP and [$^{13}C_7$]-1PE were present as minor isotopologues, their formation are due to the presence of L-[$^{13}C_7$]Phe in the L-[$^{13}C_9$]Phe (L-[$^{13}C_9$]Phe: L-[$^{13}C_8$]Phe: L-[$^{13}C_7$]Phe =89.6:7.2:0.2, based on analysis of LC-MS). Second possibility is that exchange reaction of deuterium occurs during the extraction processes of volatiles. To investigate it, we used SPME to collect the volatiles emitted from the flowers without the solvent extraction process (Figure S2, Supplementary Materials). It was found that [$^2H_5$]AP and [$^2H_6$]AP were detected as dominant isotopologue and minor isotopologue, respectively, in the feeding experiments of L-[$^2H_8$]Phe to the cut flowers. In addition, [$^{13}C_8$]AP and [$^{13}C_7$]AP were detected as dominant isotopologue and minor isotopologue, respectively, in the feeding experiments of L-[$^{13}C_9$]Phe to the cut tea flowers (Figure S4, Supplementary Materials). Third possibility is that exchange reaction of deuterium occurs during the feeding experiments. To investigate this point, firstly we compared the changes of nonlabeled AP in methanol and methanol-d_4, respectively. As shown in Figure S5A (Supplementary Materials), the ratio of [M] *m/z* 121 (natural abundance of ^{13}C of AP or [$^2H_1$]AP) to *m/z* 120 (AP) was slightly

increased in the AP in methanol-d_4 in contrast to in methanol, suggesting that [$^2H_6$]AP may be slightly transformed to [$^2H_5$]AP in the feeding experiments of L-[$^2H_8$]Phe to the cut flowers due to the exchange reaction. Secondly, we compared the changes of nonlabeled CA in methanol and methanol-d_4, respectively. The ratio of $[M-H]^-$ *m/z* 148.05 (natural abundance of ^{13}C of CA or [$^2H_1$]CA) to $[M-H]^-$ *m/z* 147.04 (CA) had no significant difference between CA in methanol and methanol-d_4 (Figure S5B, Supplementary Materials). Thirdly, we compared the changes of nonlabeled HPPA in methanol and methanol-d_4 respectively. The ratio of $[M-H]^-$ *m/z* 166.06 (natural abundance of ^{13}C of HPPA or [$^2H_1$]HPPA) to $[M-H]^-$ *m/z* 165.05 (HPPA) was significantly increased in the HPPA in methanol-d_4 in contrast to that in methanol (Figure S5C, Supplementary Materials). Furthermore, NMR evidences indicate that a certain percentage of hydrogen at α and β positions of HPPA are replaced by deuterium from methanol-d_4 (Figure S5D, Supplementary Materials). Fourthly, after either deuterium oxide supplement or co-supplement of nonlabeled L-Phe and deuterium oxide to the cut flowers, the ratio of *m/z* 121 (natural abundance of ^{13}C of AP or [$^2H_1$]AP) to *m/z* 120 (AP) and the ratio of *m/z* 123 (natural abundance of ^{13}C of 1PE or [$^2H_1$]-1PE) to *m/z* 122 (1PE) were significantly increased in contrast to the water treatment and nonlabeled L-Phe in water treatment as controls (Figure S6, Supplementary Materials). These evidences suggest that exchange reaction of deuterium such as from labeled HPPA lead to the formation of [$^2H_5$]AP and[$^2H_5$]-1PE in the feeding experiments of L-[$^2H_8$]Phe to the cut flowers. As the nonlabeled authentic standard 3-oxo-3-phenylpropionic acid is unavailable from the commercial sources, we did not investigate the exchange reaction of this compound. But the deuterium exchange reaction might also occur in the labeled 3-oxo-3-phenylpropionic acid due to the keto-enol tautomerization.

The CA is relatively stable in the exchange reaction (Figure S5B, Supplementary Materials).

Besides [$^{2}H_{7}$]CA, [$^{2}H_{6}$]CA was also detected in the cut flowers fed with L-[$^{2}H_{8}$]Phe (Figure 4B and Figure S7, Supplementary Materials). In addition, the [$^{13}C_{9}$]CA was detected in the cut flowers supplied with L-[$^{13}C_{9}$]Phe (Figure 4C). In some microorganisms such as *Propionibacterium freudenreichii*, L-Phe can be transaminated to PPA, which is further metabolized to PAA by a hydroxy acid dehydrogenase (Thierry and Maillard, 2002). It is well known that CA is converted from L-Phe by the widely distributed enzyme L-Phe ammonia-lyase (Boatright et al., 2004). CA can also be formed by the reduction of PPA to PAA and the dehydration of PAA, as proposed by Neish (1960). Such a pathway may have resulted in the formation of [$^{2}H_{6}$]CA in the flowers fed with L-[$^{2}H_{8}$]Phe in our study (Figure 4B and Figure S7, Supplementary Materials). Moreover, the [$^{2}H_{7}$]PPA (or [$^{13}C_{9}$]PPA) and [$^{2}H_{7}$]PAA (or [$^{13}C_{9}$]PAA) products were detected in the cut flowers fed with either L-[$^{2}H_{8}$]Phe or L-[$^{13}C_{9}$]Phe (Figures 5 and 6). It remains to be determined whether [$^{2}H_{5}$]AP and[$^{2}H_{5}$]-1PE may be derived from an alternative pathway (pathway 2, Figure 7).

To further investigate which pathway is a major pathway, AIP (Figure 7), a potent inhibitor of PAL (Appert et al., 2003; Zoń et al., 2004), was supplied to the *C. sinensis* flowers. As a consequence, AIP significantly inhibited the labeled AP and 1PE products derived from either L-[$^{2}H_{8}$]Phe or L-[$^{13}C_{9}$]Phe (Figure 8). This provides more evidences that the pathway already proposed in the fungus (Lapadatescu et al., 2000, Figure 1 and pathway 1 in Figure 7) is a major pathway leading from L-Phe to AP and 1PE in *C. sinensis* flowers.

Distributions of L-Phe, AP, and 1PE in various tissues and their changes during floral development

We investigated the distributions of L-Phe, AP, and 1PE in leaves and floral organs, and the

changes in their concentrations during floral development. Endogenous AP was not detected in the leaves of *C. sinensis*. The 1PE concentration in the leaves was 21.5±6.0 nmol/g fresh weight, which was less than the endogenous concentration of 1PE in the flowers at each developmental stage (Figure 9A). Similarly, the leaves contained lower concentrations of L-Phe (5.3±0.5 nmol/g fresh weight) than the flowers (see Figure 9A). The differences between the leaves and flowers in L-Phe concentrations may lead to the higher concentrations of AP and 1PE in the flowers compared with the leaves. Interestingly, at least one enzyme such as hydrogenase / dehydrogenase involved in the pathway leading from AP to 1PE was identified in both leaves and flowers (data not shown). This suggests that the small amount of 1PE found in the leaves may be due to the lack of available substrates such as L-Phe or AP. The AP and 1PE concentrations increased during floral development, whereas that of L-Phe decreased (Figure 9A). It remains to be determined whether this decrease in L-Phe is due to its transformation to related derivatives such as volatile phenylpropanoids/benzenoids and non volatile flavonoids.

We also found that the concentration of endogenous AP was lower than that of 1PE in the flowers at each developmental stage (Figure 9A). To investigate whether pH influences the transformation between AP and 1PE, we extracted crude enzymes and analyzed their hydrogenation and dehydrogenation activities under different pH conditions. The crude enzymes showed higher hydrogenation activity than dehydrogenation activity (Figure S8, Supplementary Materials). Furthermore, the hydrogenation activity decreased with increasing pH whereas the dehydrogenation activity increased with increasing pH (Figure S8, Supplementary Materials). Crushed *C. sinensis* flowers were found to have pH levels of 5.7-5.8. This subacid condition of the flowers may result in more hydrogenation than dehydrogenation in the transformation between AP and 1PE.

Recent studies have demonstrated that not all flower organs are equally employed in scent production, and spatial differences within a flower are quite common (Effmert et al., 2006). In general, petals are the main source of the whole flower bouquet, but other floral organs such as stamens, pistils, and sepals contribute to, or are solely responsible for, the emission of certain compounds (Effmert et al., 2006). In *C. sinensis* flowers, AP and 1PE occurred mainly in the anthers, as did the precursor L-Phe and the glycosides of 1PE (Figure 9B). These results suggest that the anther is the main site for the synthesis of these two volatile compounds. Anthers, which present the pollen, are important for the reproductive success of plants. Volatile compounds arising from anthers or pollen may function as attractants for flower pollinators. Alternatively, they may function in defense, to limit the destruction of the pollen or stamens by herbivores and/or pathogens (Dobson and Bergström, 2000).

To date, the (*R*)- and (*S*)-enantiomers of 1PE, and their conversion from ketones, have been characterized in many microorganisms (Itoh, et al., 1997; Höffken et al., 2006; Nakata et al., 2010). On the other hand there is only limited information on their occurrence in plants. In our study, (*R*)-1PE was identified as the dominant endogenous 1PE in *C. sinensis* flowers (Figure S9A, Supplementary Materials). After L-[$^2H_8$]Phe was fed to cut *C. sinensis* flowers (Figure S2, Supplementary Materials), much more (*R*)-[$^2H_5$]-1PE was detected than (*S*)-[$^2H_5$]-1PE (Figure S10A, Supplementary Materials). Also, when crude enzyme extracts from the flowers were assayed using [$^2H_5$]AP as a substrate, more (*R*)-[$^2H_5$]-1PE was detected than (*S*)-[$^2H_5$]-1PE (Figure S10B, Supplementary Materials). These results indicate the presence of one or more enzymes that are responsible for the conversion of AP to (*R*)-1PE in the flowers.

Emission of volatile compounds from C. sinensis flowers

The emission of volatile compounds is a characteristic trait of flowers of most plants. Much higher levels of AP are emitted from *C. sinensis* flowers than 1PE (Figure 9A). There are several possible explanations for this. One relates to the chemical properties of the volatile compounds. We found that AP is released from water to air more readily than 1PE (Figure S11, Supplementary Materials). The second possibility is that 1PE is readily converted to nonvolatile forms, such as glycosides of 1PE. We did find that the concentrations of 1PE glycosides increased during floral development, and that they were present mainly in the anthers and filaments (Figure 9). Thus, the glycosides had the same distribution and concentration changes as 1PE. Moreover, glycosides of (*R*)-1PE are dominant glycosides of 1PE (Figure S9C, Supplementary Materials). These results support the idea that 1PE is easily converted to its glycosidic form in *C. sinensis* flowers. Many aroma compounds occur as glycosidic precursors in plant cells, and they are more easily stored in this form. Glycosylated volatile compounds are more water soluble and less reactive than their free aglycone counterparts (Winterhalter and Skouroumounis, 1997). The third possibility relates to the oxidation-reduction between AP and 1PE (Figure S8, Supplementary Materials). More 1PE stored in the flowers may make equilibration between AP and 1PE. A fourth possible explanation for the higher rate of emission of AP from *C. sinensis* flowers relates to the toxic effects of AP. It was reported that AP is more toxic for the organism than either (*R*)- or (*S*)-1PE (Kniemeyer and Heider, 2001). The flowers may emit AP more readily than 1PE to reduce the accumulation of AP within their tissues.

Interestingly, the ratio of (*R*)- to (*S*)-1PE differed between the total endogenous 1PE and the total emitted 1PE (Figures S9A and S9B, Supplementary Materials). More than 88% of the endogenous 1PE was (*R*)-1PE (Figure S9A). In contrast, the levels of emitted (*S*)-1PE were similar to those of the emitted (*R*)-1PE (Figure S9B). It is not clear why such a difference exists

in the (*R*)- to (*S*)-1PE ratios. Since high amount of endogenous 1PE provides sufficient pool for 1PE release (Figure 9A), it remains to be determined whether it is regulated by the enantioselectivity of the enzymes involved in transformation between AP and 1PE, and/or the chiral selections of the glycosyl transferase and glycosyl hydrolase involved in conversion between 1PE and its glycosides, or due to some unknown factors. Moreover, it would be very interesting to investigate the possible ecological functions of the (*R*)- to (*S*)-1PE ratio in *C. sinensis* flowers. It has been speculated that plants will increase their emission of volatile compounds when attacked by herbivores, as a "cry for help" to attract natural enemies of the herbivores. Recent studies suggest that the insect responses are dependent on the quality of this volatile emission rather than merely the quantity of volatiles emitted (Bruce et al., 2010; Allmann and Baldwin, 2010).

Studies of the biochemistry and enzymology of floral scents have mainly concentrated on the isolation and characterization of enzymes and genes involved in the final steps of the biosynthesis of volatile compounds (Boatright et al., 2004). However, it is clear from this and other studies that the biosynthetic networks for plant volatile compounds are quite complex, and many biosynthetic pathways remain to be discovered. Our study provides evidence that AP and 1PE are derived from L-Phe in *C. sinensis* flowers. This information will be helpful for the future discovery of enzymes and genes involved in the formation of AP and 1PE, and will also contribute to the general understanding of the biochemistry of volatile phenylpropanoids/benzenoids in plants.

Acknowledgments

This work was supported by the Japanese Society for the Promotion of Science (JSPS ID NO.

P10101). The author F. Dong acknowledges the support of Japanese Government (Monbukagakusho: MEXT) Scholarship. We are also grateful to Prof. J. Zoń at Wroclaw University of Technology, in Poland for kindly providing the AIP.

References

Allmann S, Baldwin IT. Insects betray themselves in nature to predators by rapid isomerization of green leaf volatiles. Science 2010;329:1075-8.

Appert C, Zoń J, Amrhein N. Kinetic analysis of the inhibition of phenylalanine ammonia-lyase by 2-aminoindan-2-phosphonic acid and other phenylalanine analogues. Phytochemistry 2003;62:415-22.

Bailey WF, Luderer MR. Asymmetric addition of chiral methylmagnesium alkoxides to benzaldehyde. ARKIVOC 2010;viii:108-15.

Boatright J, Negre F, Chen XL, Kish CM, Wood B, Peel G, Orlova I, Gang D, Rhodes D, Dudareva N. Understanding *in vivo* benzenoid metabolism in petunia petal tissue. Plant Physiol 2004;135:1-19.

Bruce TJA, Midega CAO, Birkett MA, Pickett JA, Khan ZR. Is quality more important than quantity? Insect behavioural responses to changes in a volatile blend after stemborer oviposition on an African grass. Biol Lett 2010;6:314-7.

Dewich PM. Medicinal Natural Products: A Biosynthetic Approach (2nd Edition). John Wiley & Sons Ltd: England, 2002.

Dobson HEM, Bergström G. The ecology and evolution of pollen odors. Plant Syst Evol 2000;222:63-87.

Dudareva N, Pichersky E. Floral scent metabolic pathways: their regulation and evolution. In:

Dudareva N, Pichersky E, editors. Biology of Floral Scent. Boca Raton, London, New York: Taylor & Francis Group, 2006. p 55-78.

Effmert U, Buss D, Rohrbeck D, Piechulla B. Localization of the synthesis and emission of scent compounds within the flower. In: Dudareva N, Pichersky E, editors. Biology of Floral Scent. Boca Raton, London, New York: Taylor & Francis Group, 2006. p 105-24.

Höffken HW, Duong M, Friedrich T, Breuer M, Hauer B, Reinhardt R, Rabus R, Heider J. Crystal structure and enzyme kinetics of the (S)-specific 1-phenylethanol dehydrogenase of the denitrifying bacterium Strain EbN1. Biochemistry 2006;45:82-93.

Itoh N, Morihama R, Wang J, Okada K, Mizuguchi N. Purification and characterization of phenylacetaldehyde reductase from a styrene-Aasimilating *Corynebacterium* Strain, ST-10. Appl Environ Microbiol 1997;63:3783-8.

Kniemeyer O, Heider J. (*S*)-1-Phenylethanol dehydrogenase of *Azoarcus* sp. strain EbN1, an enzyme of anaerobic ethylbenzene catabolism. Arch Microbiol 2001;176:129-35.

Knudsen JT, Tollsten L, Bergstrom LG. Floral scents-a checklist of volatile compounds isolated by head-space techniques. Phytochemistry 1993;33:253-80.

Lapadatescu C, Giniès C, Quéré JLL, Bonnarme P. Novel scheme for biosynthesis of aryl metabolites from L-phenylalanine in the fungus *Bjerkandera adusta*. Appl Environ Microbiol 2000;66:1517-22.

Nakata Y, Fukae T, Kanamori R, Kanamaru S, Matsuda T. Purification and characterization of AP reductase with excellent enantioselectivity from *Geotrichum candidum* NBRC 4597. Appl Microbiol Biotechnol 2010;86:625-31.

Negre-Zakharov F, Long MC, Dudareva N. Floral scents and fruit aromas inspired by nature. In: Osbourn AE, Lanzotti V. Eds. Plant-derived Natural Products: Synthesis, Function, and

Application. Springer Berlin, Heidelberg, 2009. pp 405-31.

Neish AC. Biosynthetic pathways of aromatic compounds. Annu Rev Plant Physiol 1960;11:55-80.

Pichersky E, Gershenzon J. The formation and function of plant volatiles: perfumes for pollinator attraction and defense. Curr Opin Plant Biol 2002;5:237-43.

Pichersky E, Noel JP, Dudareva N. Biosynthesis of plant volatiles: nature's diversity and ingenuity. Science 2006;331:808-11.

Suan CL, Sarmidi MR. Immobilised lipase-catalysed resolution of (*R, S*)-1-phenylethanol in recirculated packed bed reactor. J Mol Catal B Enzym 2004;28:111-19.

Thierry A, Maillard MB. Production of cheese flavour compounds derived from amino acid catabolism by *Propionibacterium freudenreichii*. Lait 2002;82:17-32.

Winterhalter P, Skouroumounis GK. Glycoconjugated aroma compounds: Occurrence, role and biotechnological transformation. In: Berger RG, Ed. "Advances in Biochemical Engineering/Biotechnology", Biotechnology of Aroma Compounds. Springer Berlin, Heidelberg, 1997;55:73-105.

Yun H, Yang YH, Cho BK, Hwang BY, Kim BG. Simultaneous synthesis of enantiomerically pure (*R*)-1-phenylethanol and (*R*)-α-methylbenzylamine from racemic α-methylbenzylamine using ω-transaminase/alcohol dehydrogenase/glucose dehydrogenase coupling reaction. Biotech Lett 2003;25:809-14.

Zoń J, Amrhein N. Inhibitors of phenylalanine ammonia-lyase: 2-aminoindan-2-phosphonic acid and related compounds. Liebigs Ann Chem 1992;6:625-8.

Zoń J, Szefczyk B, Sawka-Dobrowolska W, Gancarz R, Kucharska-Zoń M, Latajka R, Amrhein N, Miziak P, Szczepanik W. Experimental and *ab initio* calculated structures of 2-

aminoindane-2-phosphonic acid, a potent inhibitor of phenylalanine ammonia-lyase, and theoretical studies of its binding to the model enzyme structure. New J Chem 2004;28:1048-55.

Figure Legends

Figure 1 Proposed pathway of AP derived from L-Phe in the fungus (Ref: Lapadatescu et al., 2000).

Figure 2 Mass chromatograms of endogenous labeled AP and 1PE in *C. sinensis* flowers supplied with L-[$^{2}H_{8}$]Phe.
[M], [M-CH_3], and [M-$OCCH_3$] are characteristic ions of nonlabeled AP, and [M], [M-CH_3], and [M-$OHCHCH_3$] are characteristic ions of nonlabeled 1PE in GC-MS analysis. The fragments of labeled AP and 1PE were assigned based on the pattern of nonlabeled AP and 1PE.

Figure 3 Mass chromatograms of endogenous labeled AP and 1PE in *C. sinensis* flowers supplied with L-[$^{13}C_{9}$]Phe.
[M], [M-CH_3], and [M-$OCCH_3$] are characteristic ions of nonlabeled AP, and [M], [M-CH_3], and [M-$OHCHCH_3$] are characteristic ions of nonlabeled 1PE in GC-MS analysis. The fragments of labeled AP and 1PE were assigned based on the pattern of nonlabeled AP and 1PE.

Figure 4 Measurements of labeled CA in *C. sinensis* flowers supplied with L-[$^{2}H_{8}$]Phe (B) and L-[$^{13}C_{9}$]Phe (C), respectively, based on analysis of GC-MS-SIM.
(A) [M], [M-CH_3], and [M-$OSi(CH_3)_3$] are characteristic ions of authentic standard nonlabeled CA-MSTFA derived product (See Table S1). (B and C) The controls were untreated cut flowers. The fragments of labeled CA- MSTFA derived products were assigned based on the pattern of nonlabeled standard CA-MSTFA derived product.

Figure 5 Measurements of labeled PPA in *C. sinensis* flowers supplied with L-[$^{2}H_{8}$]Phe (B) and L-[$^{13}C_{9}$]Phe (C), respectively, based on analysis of GC-MS-SIM.
(A) [M], [M-CH_3], and [M-$OSi(CH_3)_3$] are characteristic ions of authentic standard nonlabeled PPA-MSTFA derived product (See Table S1). The characteristic ion at *m/z* 90 was also identified. (B and C) The controls were untreated cut flowers. The fragments of labeled PPA- MSTFA derived products were assigned based on the pattern of nonlabeled standard PPA-MSTFA derived product. (C) Although a small peak of ion at *m/z* 97 was also detected in control, the ^{13}C labeled PPA- MSTFA derived product could also be confirmed based on the characteristic ions of [M], [M-CH_3], and [M-$OSi(CH_3)_3$].

Figure 6 Measurements of labeled PAA in *C. sinensis* flowers supplied with L-[$^{2}H_{8}$]Phe (B) and L-[$^{13}C_{9}$]Phe (C), respectively, based on analysis of GC-MS-SIM.
(A) [M-CH_3] and [M-$OSi(CH_3)_3$] are characteristic ions of authentic standard nonlabeled PAA-MSTFA derived product (See Table S1). The [M] ion was not detected in the GC-MS-SIM. The fragment at *m/z* 91 was identified to investigate whether the [$^{2}H_{7}$]PAA product is [α,β,2,3,4,5,6-$^{2}H_{7}$]PAA or [β,β,2,3,4,5,6-$^{2}H_{7}$]PAA after supplement of L-[$^{2}H_{8}$]Phe to cut flowers. (B and C) The controls were untreated cut flowers. The fragments of labeled PAA-MSTFA derived products were assigned based on the pattern of nonlabeled standard PAA-MSTFA derived product.

Figure 7 Hypothetical pathways for the formation of [$^{2}H_{5}$] and [$^{2}H_{6}$]AP and 1PE derived from L-[$^{2}H_{8}$]Phe supplied to *C. sinensis* flowers.
The compounds enclosed in rectangles were examined in the present study. We have not yet

detected labeled HPPA products in flowers fed with either L-[$^{2}H_{8}$]Phe or L-[$^{13}C_{9}$]Phe. This may be due to its occurrence in trace amounts in *C. sinensis* flowers, or its easy transformation to other metabolites. # The deuterium exchange reaction might also occur in the labeled 3-oxo-3-phenylpropionic acid due to the keto-enol tautomerization.

Figure 8 Inhibitions of labeled AP and 1PE products derived from L-[$^{2}H_{8}$]Phe (A) and L-[$^{13}C_{9}$]Phe (B) by AIP in *C. sinensis* flowers.

The individual labeled L-Phe treatment was defined as 100%. (A) The relative ratio of [$^{2}H_{5\text{-}6}$]AP was calculated based on sum of peak area at *m/z* 82 and 110. The relative ratio of [$^{2}H_{5\text{-}6}$]-1PE was calculated based on sum of peak area at *m/z* 82 and 112. (B) The relative ratio of [$^{13}C_{8}$]AP was calculated based on sum of *m/z* 83 and 112. The relative ratio of [$^{13}C_{8}$]-1PE was calculated based on sum of *m/z* 83 and 114.

Figure 9 Changes in metabolites during floral development (A) and their distributions (B) in floral organs of *C. sinensis.*

The data are expressed as means ± S.D. (n=3). (A) Emission, volatiles emitted from the flowers, which were collected by Montrap absorption system. Pool, endogenous volatiles in the flowers, which were extracted by organic solvent. (B) The fully open flowers were divided into four parts including petals, filaments, anthers, and other parts. The “other parts” are a mixture of carpels, receptacles, sepals, and pedicels. The biomass contributions of petals, filaments, anthers, and other parts to 1 flower are 42%, 26.4%, 18%, and 13.4%, respectively. The relative ratio (%) of each metabolite was calculated based on the contribution of each floral organ to 1 fully open flower.

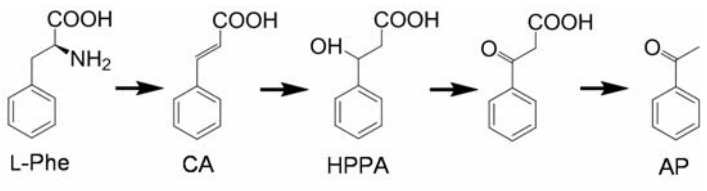

Figure 1 Fang DONG

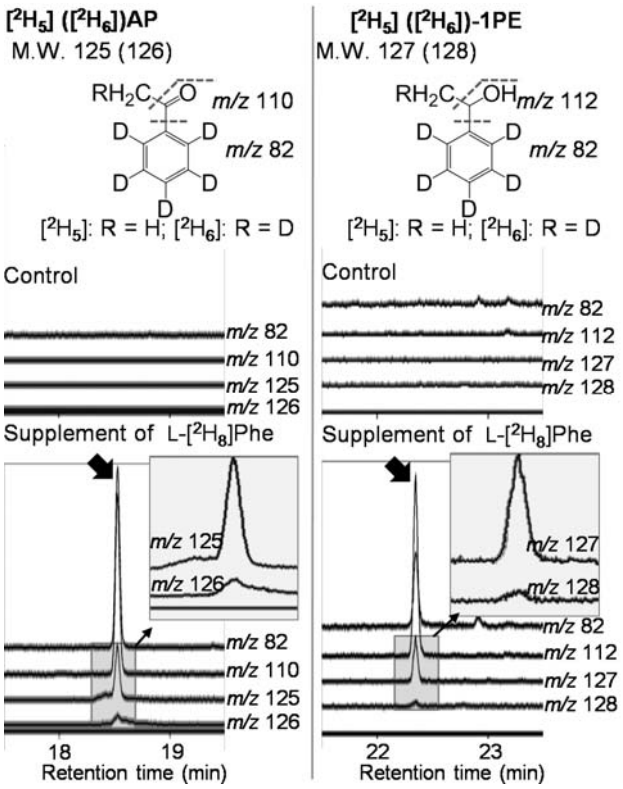

Figure 2 Fang DONG

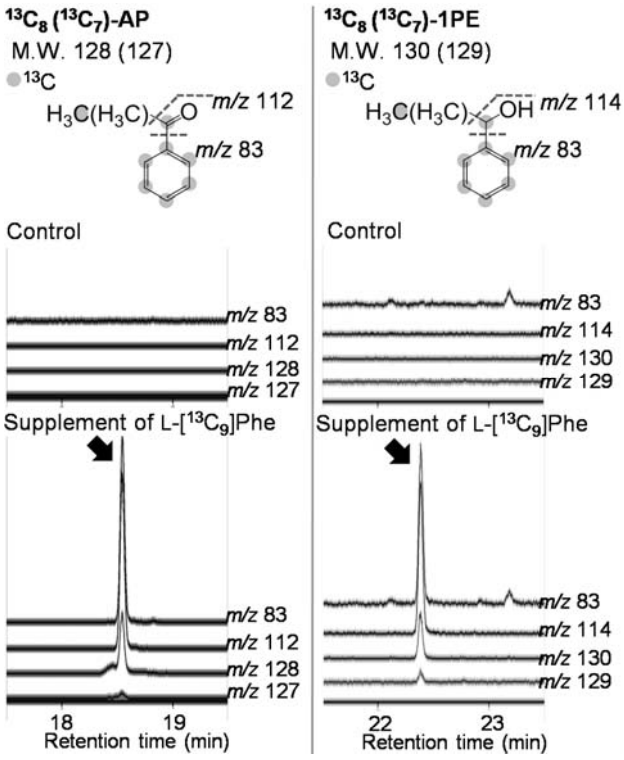

Figure 3 Fang DONG

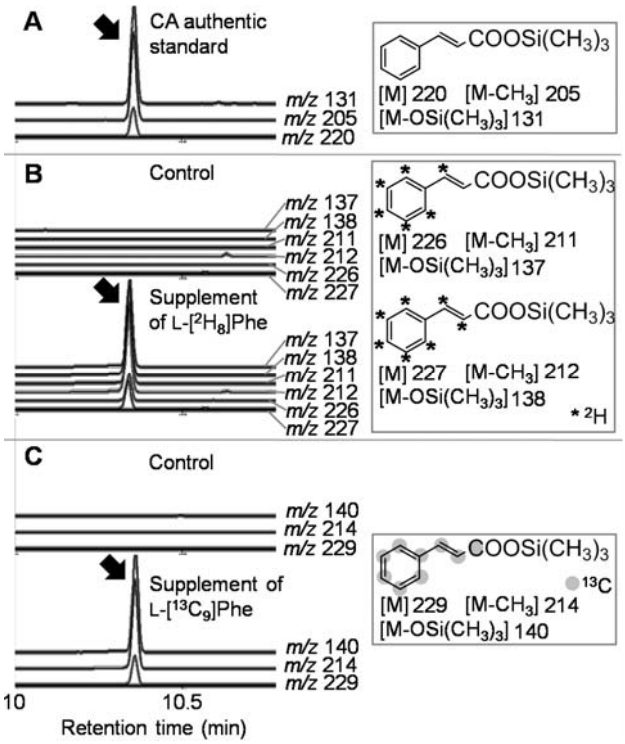

Figure 4 Fang DONG

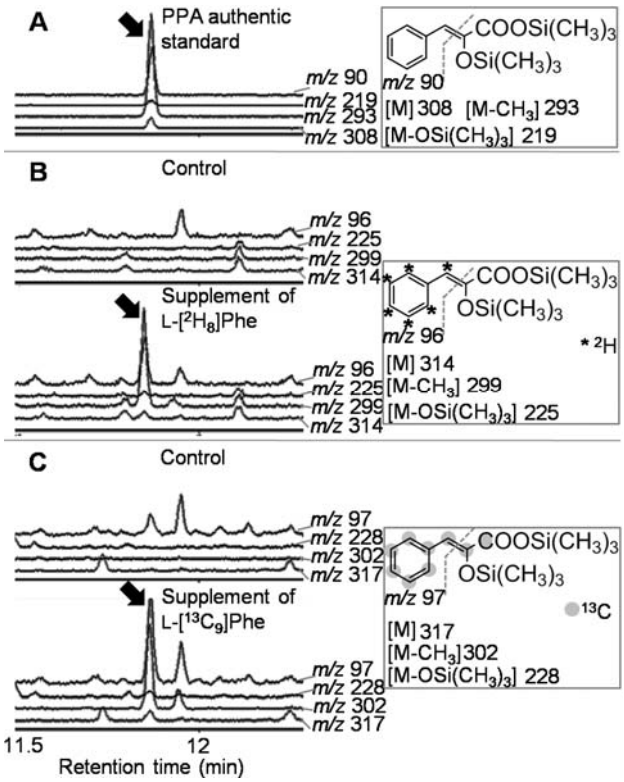

Figure 5 Fang DONG

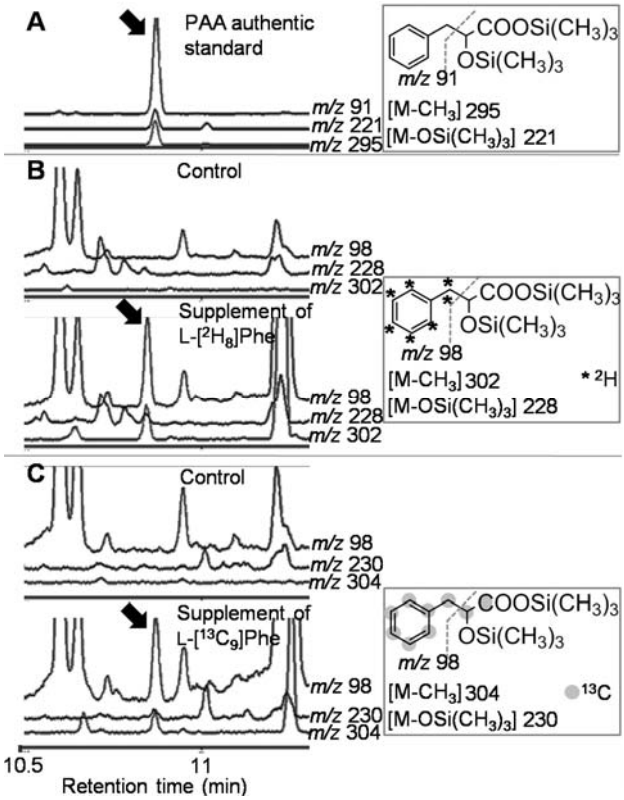

Figure 6 Fang DONG

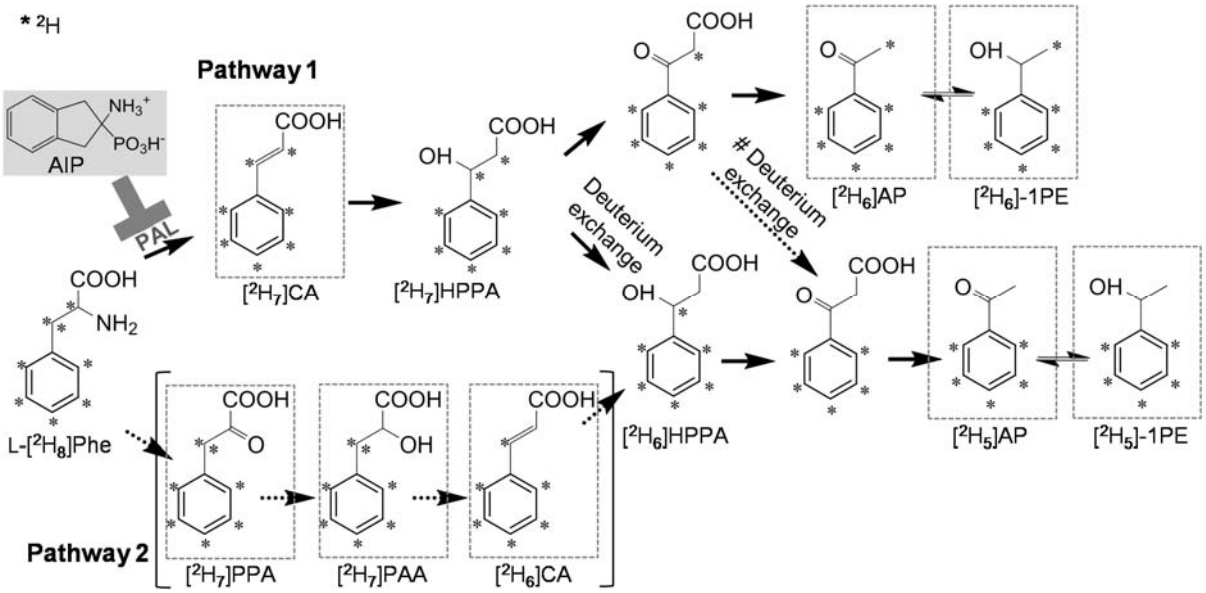

Figure 7 Fang DONG

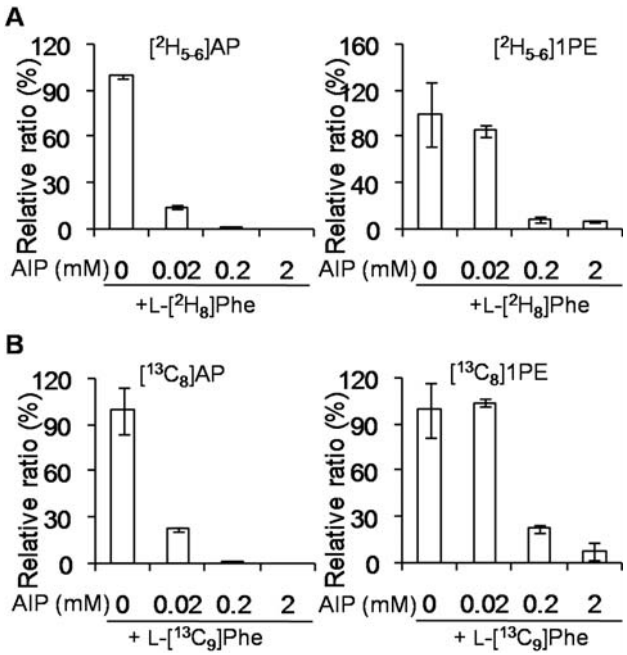

Figure 8 Fang DONG

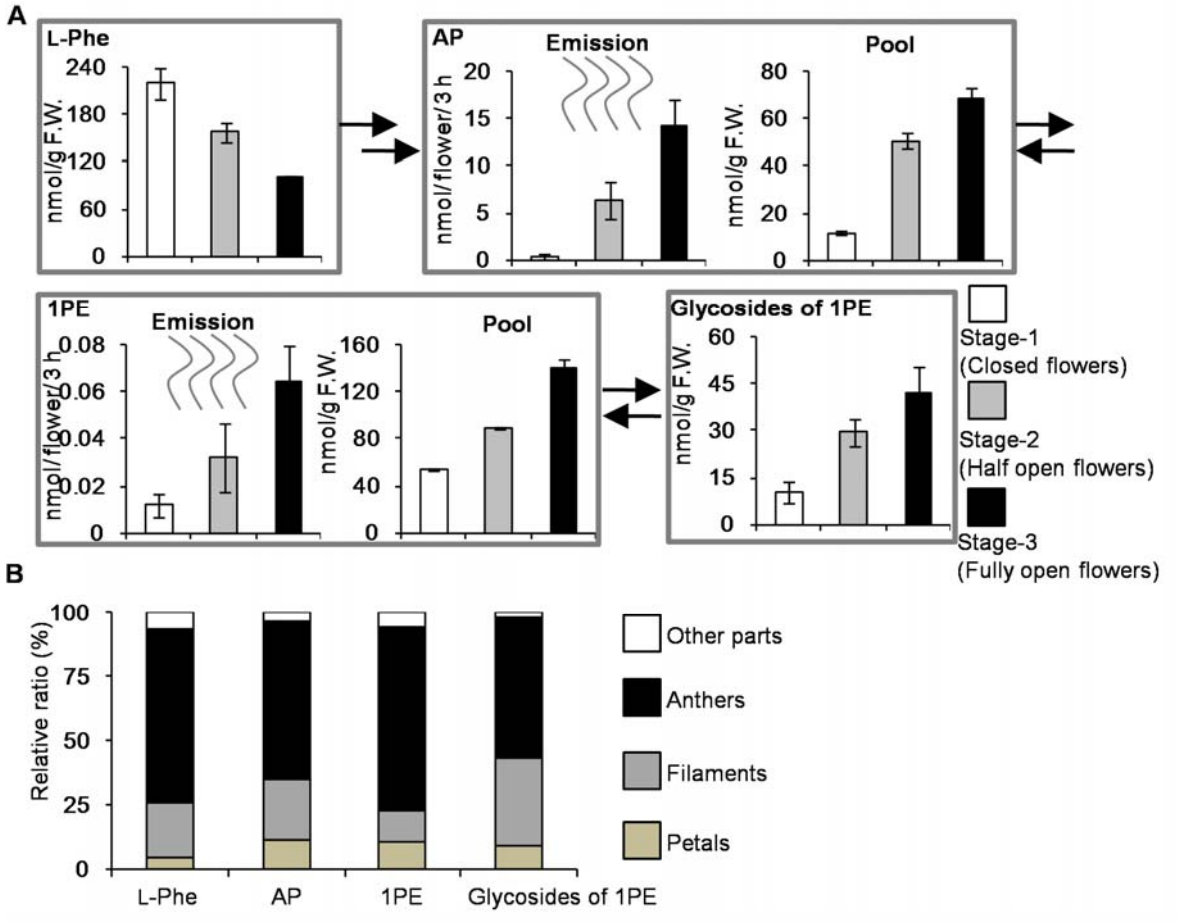

Figure 9 Fang DONG

Supplementary Materials

Table S1 MSTFA derived products of nonlabeled authentic standards and their molecular weights, and characteristic ions based on analysis of GC-TOFMS

Metabolite	MSTFA derived product	R.T. (min)	M.W.	Characteristic ions			
				M	M-CH_3	M-$OSi(CH_3)_3$	
trans-cinnamic acid 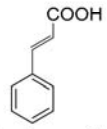	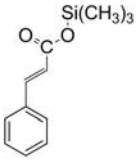	8.95-9.10	220.092	220.092	205.0685	131.0497	(Calculated)
				220.09	205.06	131.05	(Detected)
3-hydroxy-3-phenylpropionic acid 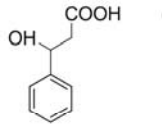	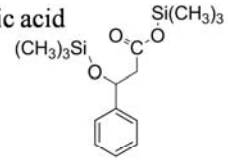	9.38-9.45	310.142	310.142	295.1186	221.0998	(Calculated)
				310.10	295.12	221.10	(Detected)
phenyllactic acid 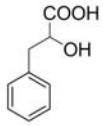	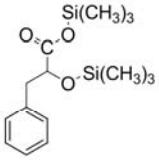	9.32-9.39	310.142	310.142	295.1186	221.0998	(Calculated)
				N.D.	295.12	221.09	(Detected)
phenylpyruvic acid 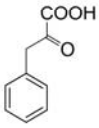	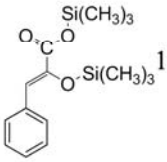	10.25-10.31	308.1264	308.1264	293.1029	219.0841	(Calculated)
				308.13	293.1	219.05	(Detected)

N.D., not detected. The nonlabeled authentic standards were derivatized with 70 μL of MSTFA at 37°C for 60 min. The MSTFA derivates were then analyzed by GC-TOFMS using a JEOL AccuTOF™ mass spectrometer, and the system was controlled by a MassCenter software. The injector temperature was 240°C, splitless mode was used with a splitless time of 1 min, and helium was the carrier gas with a velocity of 1.2 mL/min. The GC was equipped with a HP-5 column (Agilent Technologies, 30 m × 0.32 mm × 0.25 μm). The column temperature was held at 80°C for 2 min, ramped at 15°C/min to 280°C, then kept at this temperature for 20 min. The MS detector was operated in mass range *m/z* 50–500.

Table S2 Concentrations of endogenous AP and 1PE in *C. sasanqua* flowers and *C. sinensis* flowers

Flowers [a]		AP (nmol/g F.W. [c])		1PE (nmol/g F.W.)	
		Closed flowers	Fully-open flowers	Closed flowers	Fully-open flowers
C. sasanqua	White	4.38 ± 0.16 [b]	6.65 ± 0.41	N.D.	5.18 ± 0.25
	Red	N.D.[c]	29.41± 0.29	N.D.	3.61 ± 0.36
C. sinensis		11.64 ± 0.47	68.07 ± 4.46	54.57 ± 0.84	139.33 ± 7.82

[a] The flowers were collected in Shizuoka, Japan in November and December, 2009. [b] Data are expressed as mean ± S.D. (n=3). [c] N.D., Not detected; F.W., fresh weight.

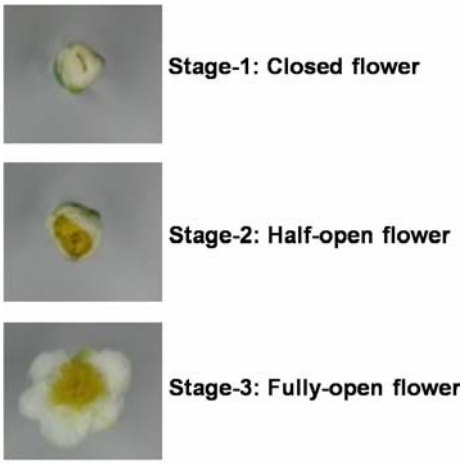

Figure S1 Flowers of *C. sinensis* var. Yabukita at stages 1-3.

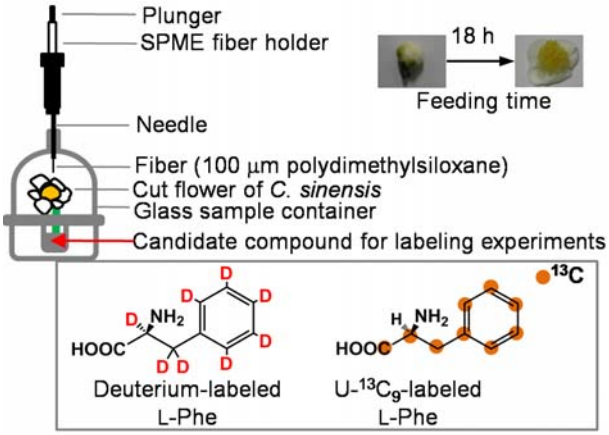

Figure S2 Design for the feeding experiment in which L-[$^{2}H_{8}$]Phe and L-[$^{13}C_{9}$]Phe were supplied to cut flowers of *C. sinensis*, respectively.

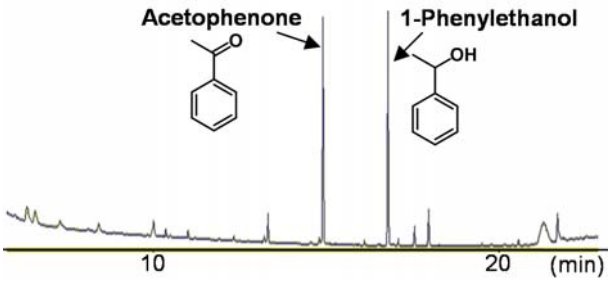

Figure S3 Total ion chromatogram of endogenous volatile compounds of *C. sinensis* var. Yabukita at stage 3.

The SUPELCOWAX^{TM} 10 column (Supelco Inc., 30 m × 0.25 mm × 0.25 μm) was used. Helium was used as a carrier gas with a flow of 1.5 mL/min. The GC oven was maintained at 40°C for 3 min, and the temperature of the oven was programmed at 10°C/min to 220°C, 30°C/min to 240°C and kept at this temperature for 3 min. The MS analyses were carried out in full scan (mass range *m/z* 50–280).

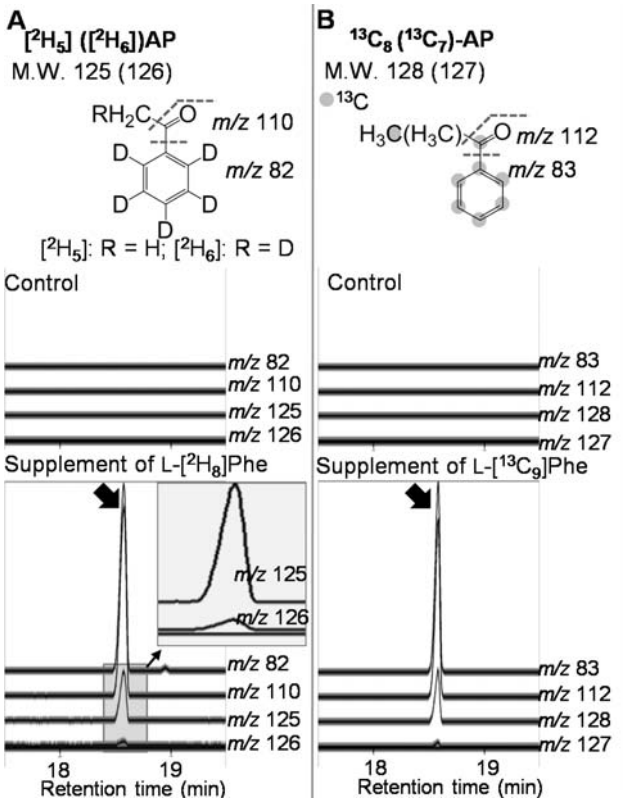

Figure S4 Mass chromatograms of labeled AP emitted from *C. sinensis* flowers supplied with L-[$^{2}H_{8}$]Phe (A) and L-[$^{13}C_{9}$]Phe (B), respectively.

The volatiles were collected by SPME as shown in the Figure S2. [M], [M-CH_3], and [M-$OCCH_3$] are characteristic ions of nonlabeled AP in GC-MS analysis. The fragments of labeled AP were assigned based on the pattern of nonlabeled AP.

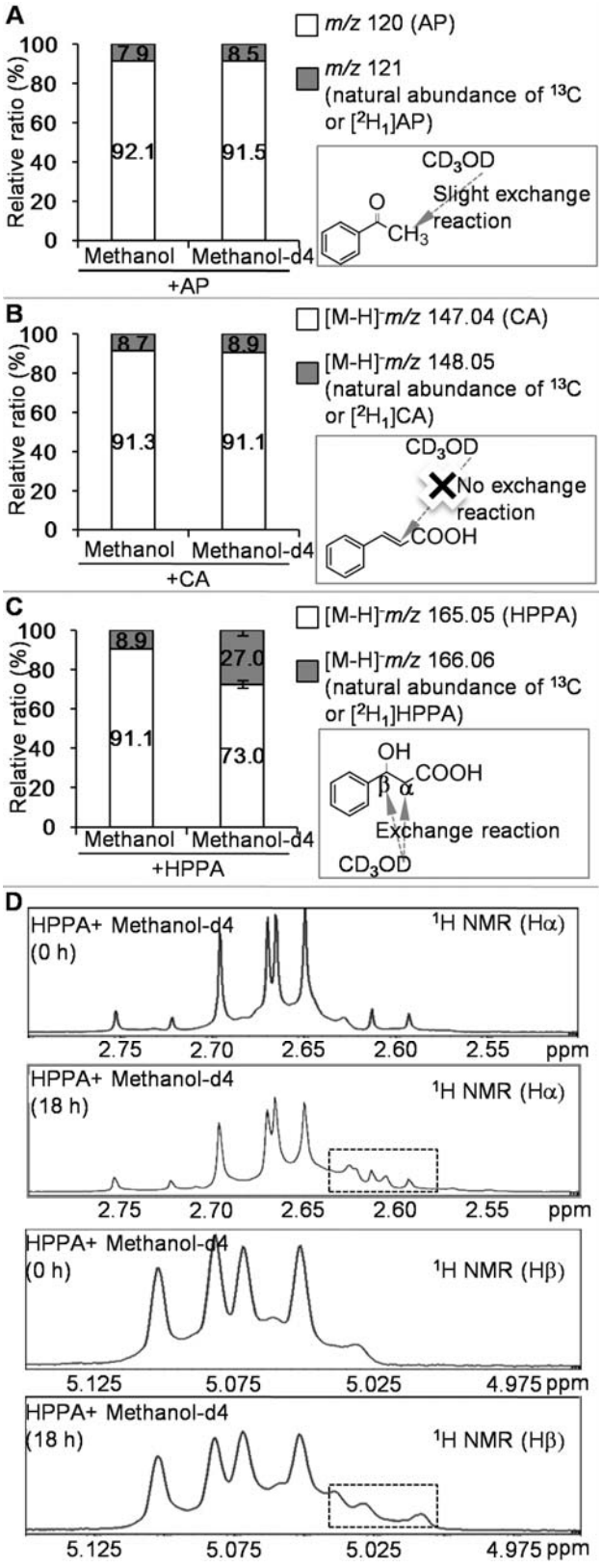
A
m/z 120 (AP)
m/z 121
(natural abundance of 13C
or [2H1]AP)
Relative ratio (%)
100
80
60
40
20
0
7.9
8.5
92.1
91.5
Methanol
Methanol-d4
+AP
CD3OD
Slight exchange
reaction
O
CH3
B
[M-H]- m/z 147.04 (CA)
[M-H]- m/z 148.05
(natural abundance of 13C
or [2H1]CA)
8.7
8.9
91.3
91.1
Methanol
Methanol-d4
+CA
CD3OD
No exchange
reaction
COOH
C
[M-H]- m/z 165.05 (HPPA)
[M-H]- m/z 166.06
(natural abundance of 13C
or [2H1]HPPA)
8.9
27.0
91.1
73.0
Methanol
Methanol-d4
+HPPA
OH
COOH
β α
Exchange reaction
CD3OD
D
HPPA+ Methanol-d4
(0 h)
1H NMR (Hα)
2.75
2.70
2.65
2.60
2.55
ppm
HPPA+ Methanol-d4
(18 h)
1H NMR (Hα)
HPPA+ Methanol-d4
(0 h)
1H NMR (Hβ)
5.125
5.075
5.025
4.975 ppm
HPPA+ Methanol-d4
(18 h)
1H NMR (Hβ)

Figure S5 Investigations on exchange reaction of deuterium of AP (A), CA (B), and HPPA (C and D) in methanol and methanol-d_4, respectively.

The relative ratio (%) was calculated based on the peak area of each ion. (A) The AP was analyzed by GC-MS. (B and C) The CA and HPPA were analyzed by LC-TOFMS. (D) The HPPA was analyzed by ^{1}H NMR (270 MHz). The coupling marked in dotted rectangles indicated the occurrence in the lower frequency shift and couplings due to the replacement of one of the ^{1}H with a ^{2}H at α- and β-positions. In addition, intensities of ^{1}H at α- and β-position of HPPA were decreased by 3.8% and 18.5%, respectively, after 18 h-incubation in methanol-d_4. These suggest that a certain percentage of ^{1}H at α- and β-position were replaced by ^{2}H of methanol-d_4.

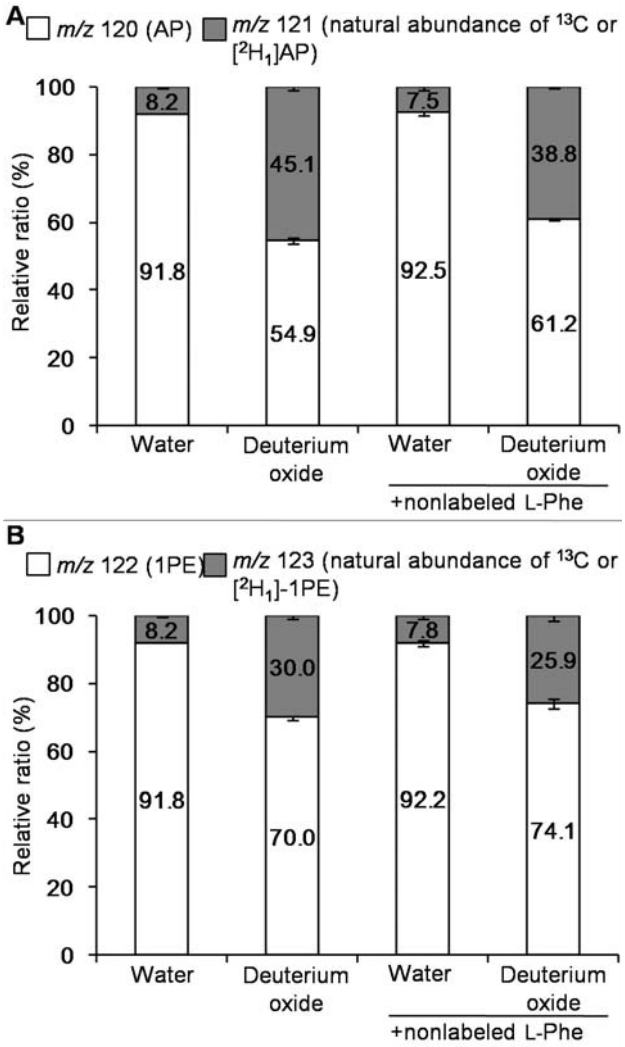

Figure S6 Investigations on exchange reaction of deuterium of AP (A) and 1PE (B) in the feeding experiments of nonlabeled L-Phe and deuterium oxide to cut flowers.

Water treatment and nonlabeled L-Phe in water treatment are controls. The relative ratio (%) was calculated based on the peak area of each ion. The AP and 1PE were analyzed by GC-MS.

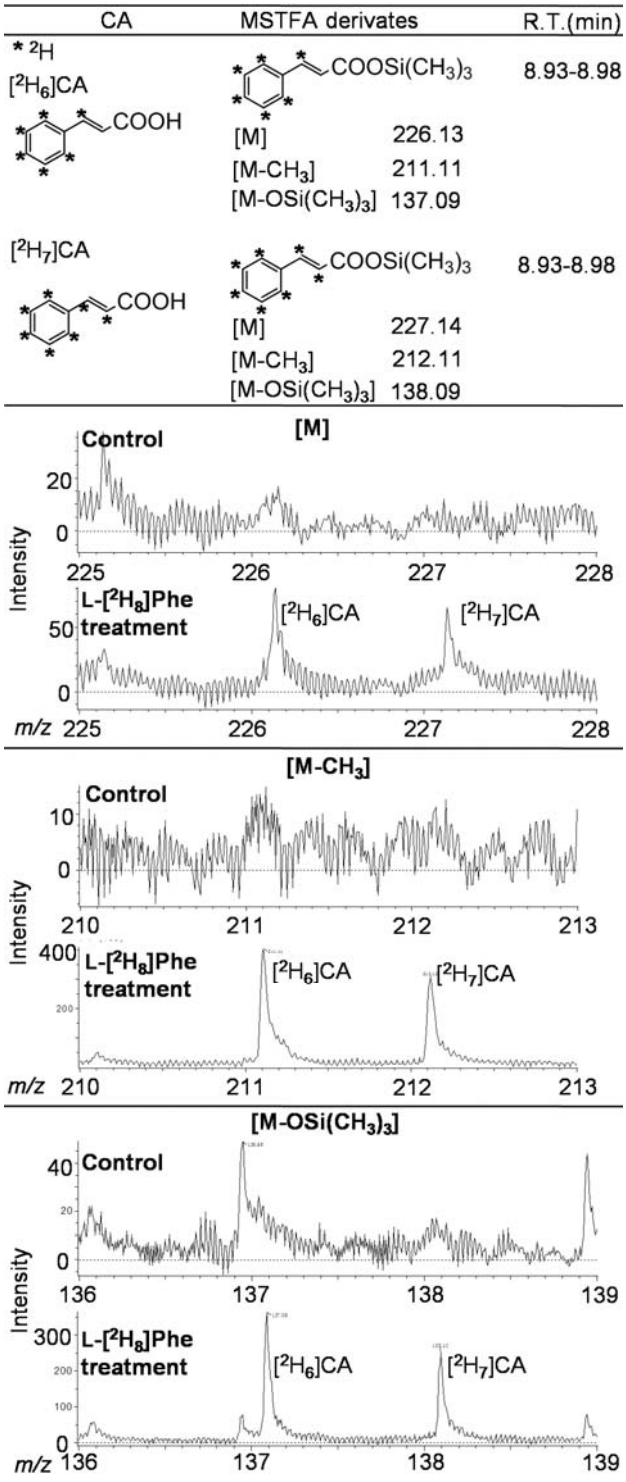

Figure S7 Measurements of [$^2H_6$] and [$^2H_7$]CA in *C. sinensis* flowers supplied with L-[$^2H_8$]Phe.

The controls were untreated cut flowers. The retention times (R.T.) and fragmentation patterns of the [$^2H_6$]CA and [$^2H_7$]CA are consistent with those of the nonlabeled authentic CA standard (R.T. 8.95-9.10 min). 160 mg (fresh weight)

of floral tissues were crushed to a fine powder using a Multi-Beads Shocker (2,000 rpm, 15 sec), then extracted with 1 mL of cold methanol by vortexing for 2 min followed by an ultrasonic extraction in ice cold water for 10 min. Each extract was mixed with 1 mL of cold chloroform and 0.4 mL of cold water for phase separation, and the resulting upper layer was removed, filtered through a 0.2 μm membrane filter, dried, and derivatized with 70 μL of MSTFA at 37°C for 60 min. The MSTFA derivates were then analyzed by GC-TOFMS as described in Table S1.

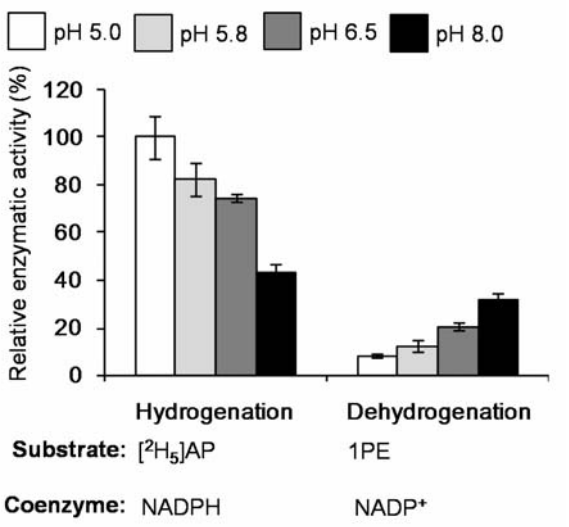

Figure S8 Effects of pH on hydrogenation and dehydrogenation by crude enzymes extracted from *C. sinensis* flowers.

The hydrogenation activity at pH 5.0 was set at 100%. The data are expressed as means ± S.D. (n=3).

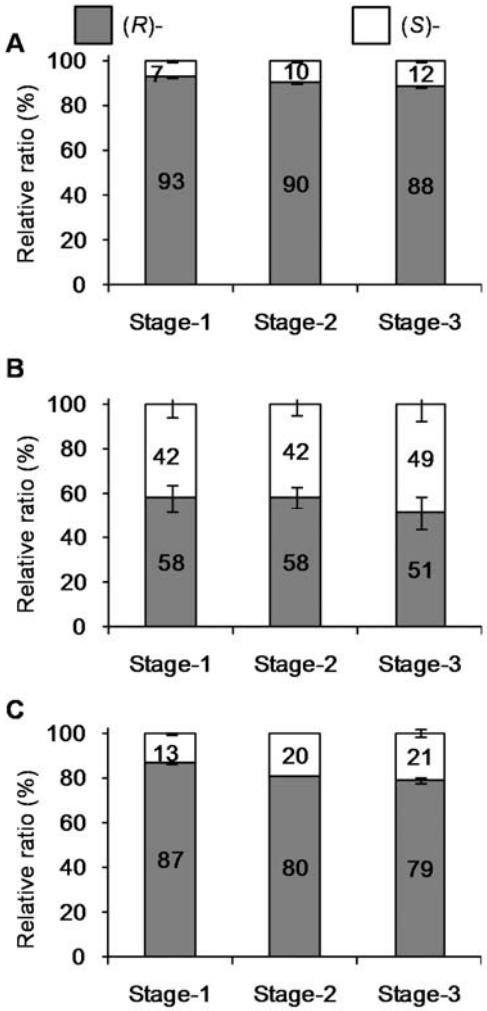

Figure S9 Ratios of (*R*)- to (*S*)-1PE in the endogenous 1PE (A), the emitted 1PE (B), and the glycosides of 1PE (C) during floral development.

The data are expressed as means ± S.D. (n=3).

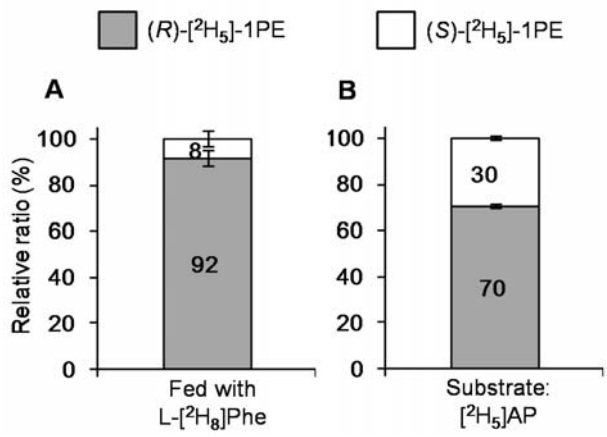

Figure S10 Ratio of (*R*)- to (*S*)-[$^2H_5$]-1PE in cut *C. sinensis* flowers fed with L-[$^2H_8$]Phe (A), and in a crude enzyme assay with [$^2H_5$]AP as the substrate (B).

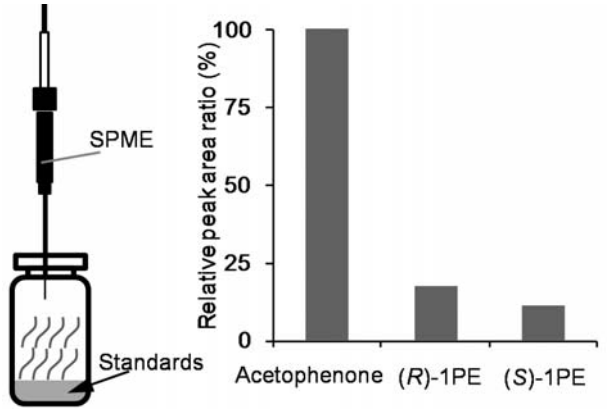

Figure S11 Emission of authentic standards of AP and 1PE from water.

The concentrations of the authentic standards were 100 nmol in 1 mL water. The emitted volatile compounds were collected by solid phase microextraction for 60 min. The amount of AP emitted from the water was set at 100%.